Bending vibration of cantilevered thin-walled beams subjected to time-dependent external excitations

Ohseop Song
Mechanical Engineering Department, Choong-Nam National University, Taejon, 305-764, Korea

Liviu Librescu
Engineering Science and Mechanics Department, Virginia Polytechnic Institute and State University, Blacksburg, Virginia 24061-0219

(Received 27 June 1994; revised 11 January 1995; accepted 15 February 1995)

The bending vibration of cantilevered thin-walled beams of arbitrary closed cross section exposed to time-dependent external excitations is investigated. The beam model used in this study incorporates a number of nonclassical effects, namely, transverse shear, secondary warping, anisotropy of constituent materials, and heterogeneity of the construction. An exact methodology based on the Laplace transform technique aiming at determining the frequency-response characteristics is used, and numerical illustrations emphasizing the effects of a number of geometrical and mechanical parameters on the frequency response behavior are displayed. © *1995 Acoustical Society of America.*

PACS numbers: 43.40.Cw

INTRODUCTION

A great deal of interest for a better understanding of the response behavior of composite structures subjected to time-dependent external excitations is manifested in the literature. This interest is due to the increased use of advanced composite materials in the various fields of the modern technology. Due to their exotic properties, the advanced composite material structures are likely to play a great role in the construction of the next generation of aeronautical and aerospace vehicles, as well as of naval constructions. In spite of the evident importance, to the best of the authors' knowledge, with the exception of studies by Bank and Kao[1] and Lee and Chao,[2] the main body of the research was devoted entirely to study the response behavior of composite structures modeled as plate and shells (see, e.g., Ref. 3). Little work has been done toward the study of the response behavior of thin-walled beams in general and of their counterparts, with closed cross-section contours, in particular. The absence of such results is more intriguing as this structural model is basic when dealing with a number of important constructions such as airplane wing and fuselage, helicopter and turbine blades, tilt rotor aircraft, as well as many other ones widely used in mechanical engineering. This paper is devoted to this topic.

I. STATEMENT OF THE PROBLEM: BASIC ASSUMPTIONS

The case of cantilevered thin-walled beams of arbitrary closed cross section is considered. It is assumed that the beam is symmetrically composed of transversely isotropic material layers (the surface of isotropy being parallel to the reference surface of the beam structure). This implies that the structure exhibits both a geometrical and physical symmetry across its thickness.

Two coordinate systems are used in the forthcoming developments: (i) a *global* Cartesian orthogonal (x,y,z) one, where (x,y) denote the cross-section beam coordinates and z the spanwise coordinate, and (ii) a *local* orthogonal system (n,s,z) where n and s denote the thicknesswise coordinate normal to the beam midsurface and the tangential one along the contour line of the beam cross section, respectively (see Fig. 1).

In order to substantiate the theoretical beam model the following assumptions are adopted:[3–8]

(1) The cross sections of the beam do not deform in their own planes.

(2) The transverse shear flexibility exhibited by the advanced composite material systems is taken into consideration.

(3) The hoop stress resultant N_{ss} is considered negligibly small with respect to the remaining ones.

(4) As a result of the considered anisotropy of the material layers, of the symmetry of the structure and of the assumption that the external loads are distributed along the beam z axis only, an exact decoupling of transverse bending (flapping) (expressed in terms of variables v_0 and θ_x), lateral bending (lagging) (expressed in terms of u_0 and θ_y), and twist (in terms of ϕ) is obtained. Herein, we will confine ourselves to the transverse bending (flapping) motion only.

Having in view the importance of the secondary warping effect (see in this sense the monograph by Gjelsvik[8] where the physical significance of this effect is clearly emphasized) and since secondary warping induces transverse bending, this effect will be also considered. As a result of the incorporation of the transverse shear effect, the analysis developed herein could also accommodate the case of thick-walled beams for which case $h_{\max}/b \geq 0.1$ where $h_{\max}$ denotes the maximum thickness of the beam, b denoting a typical cross-sectional dimension. In spite of this, the standard terminology of *thin-walled beams* will still be used.

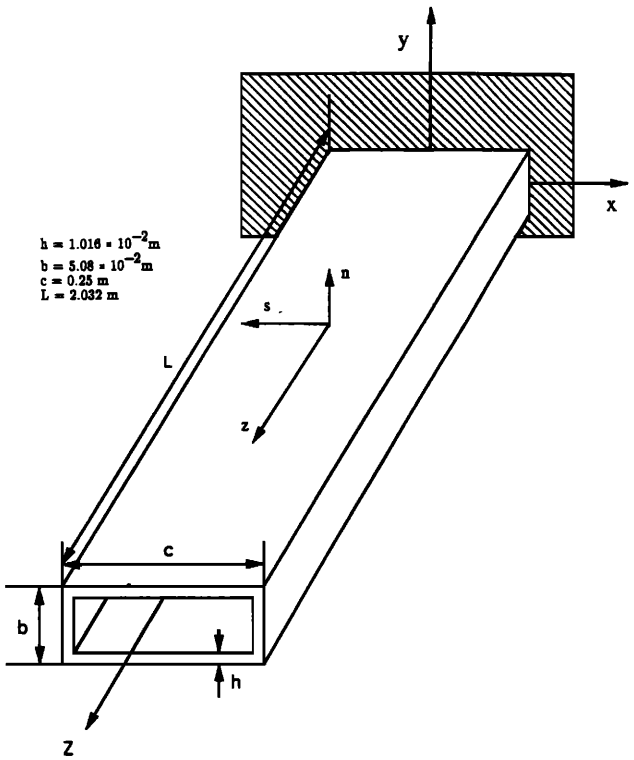

FIG. 1. Geometry of the cantilevered box-beam (not to scale).

II. EQUATIONS OF MOTION: BOUNDARY CONDITIONS

The equations of undamped motion and the associated boundary conditions of thin-walled beams can be obtained via Hamilton's variational principle.[5–7] The equations of motion associated with the transverse bending constitute a part of the general equations of motion as derived in Refs. 6 and 7. These are

$$\delta v_0 : Q_y' + p_y = I_1, \tag{1a}$$

$$\delta \theta_x : M_x' - Q_y = I_2. \tag{1b}$$

Here $p_y[\equiv p_y(z;t)]$ denotes the transverse distributed loading; I_1 and I_2 denote the inertia terms defined as[6]

$$I_1 = \ddot{v}_0 \oint m_0 \, ds, \tag{2a}$$

$$I_2 = \ddot{\theta}_x \oint \left[m_0 y^2 + m_2 \left(\frac{dx}{ds} \right)^2 \right] ds, \tag{2b}$$

where

$$(m_0, m_2) = \sum_{k=1}^{N} \int_{h_{(k-1)}}^{h_{(k)}} \rho_{(k)} (1, n^2) dn \tag{3}$$

denotes the mass terms. In addition, $v_0[\equiv v_0(z;t)]$ and $\theta_x[\equiv \theta_x(z;t)]$ denote the transverse displacement and the rotation about the x axis, respectively, N denotes the number of constituent layers, $\oint(\,)ds$ denotes the integral along the closed midline contour, $\rho_{(k)}$ denotes the mass density of the kth layer, while the primes and overdots denote derivative with respect to the z coordinate and time t, respectively. In Eqs. (1), Q_y and M_x denote the transverse shear force in the y direction, and the bending moment about the x axis, respectively. As obtained in Refs. 6 and 7 they are defined as

$$Q_y(z;t) = \oint \left(N_{sz} \frac{dy}{ds} - N_{zn} \frac{dx}{ds} \right) ds, \tag{4a}$$

$$M_x(z;t) = \oint \left(y N_{zz} - L_{zz} \frac{dx}{ds} \right) ds, \tag{4b}$$

where N_{zz}, N_{sz}, and N_{zn} denote the local spanwise, tangential shear, and transverse shear stress resultants, respectively, while L_{zz} denotes the local stress couple. Their expression in terms of strain components can be found in Ref. 7.

Based on the equations of motion (1), on the constitutive equations associated with Q_y and M_x and on the geometric equations correlating the strain measures with the displacement quantities,[6,7] the equations governing the bending motion are obtained as

$$a_{55}(v_0'' + \theta_x') + p_y = b_1 \ddot{v}_0, \tag{5a}$$

$$a_{33}\theta_x'' - a_{55}(v_0' + \theta_x) = b_2 \ddot{\theta}_x. \tag{5b}$$

Here the *global* stiffness quantities a_{33} and a_{55} are expressed as

$$a_{33} = \oint \left[K_{11} y^2 + K_{44} \left(\frac{dx}{ds} \right)^2 \right] ds, \tag{6a}$$

$$a_{55} = \oint \left[A_{66} \left(\frac{dy}{ds} \right)^2 + A_{44} \left(\frac{dx}{ds} \right)^2 \right] ds, \tag{6b}$$

where

$$K_{11} = A_{11} - \frac{A_{12}^2}{A_{11}}, \tag{7a}$$

$$K_{44} = D_{11} \equiv D, \tag{7b}$$

denote the *local* stiffness quantities, A_{ij} $(i,j = 1,2,6)$ and D denote *local* membrane and bending stiffness quantities, while A_{44} denotes the *local* transverse shear stiffness. They are defined in a generic form as

$$A_{ij} = \sum_{k=1}^{N} C_{ij}^{(k)} (n_{(k)} - n_{(k-1)}), \tag{8a}$$

$$D_{ij} = \frac{1}{3} \sum_{k=1}^{N} C_{ij}^{(k)} (n_{(k)}^3 - n_{(k-1)}^3). \tag{8b}$$

where the index (k) accompanying a certain quantity identifies its affiliation to the kth layer.

In the evaluation of stiffness quantities (8) and implicitly of the ones given by Eqs. (6) and (7), one should have in view that associated with a transversely isotropic material, the nonzero elastic coefficients expressed in terms of the engineering constants are as (see Ref. 9)

$$\begin{aligned} &C_{11} = (E\nu'^2 - E')E/\Delta, \quad C_{12} = -(E\nu'^2 + E'\nu)E/\Delta, \\ &C_{13} = -\nu'(1+\nu)EE'/\Delta, \quad C_{33} = -(1-\nu^2)E'^2/\Delta, \\ &(C_{11} - C_{12})/2 = G[\equiv E/2(1+\nu)]. \end{aligned} \tag{9}$$

In Eqs. (9), Δ is expressed as $\Delta=(1+\nu)(2E\nu'^2+E'\nu-E')$, E, ν and E', ν' denote Young's moduli and Poisson's ratios associated with the surface of isotropy and transverse to the surface of isotropy, respectively, while G and G' denote the tangential and transverse shear moduli, respectively. For a single layered construction, the mass terms b_1 and b_2 are

$$b_1=\oint \rho h\, ds, \tag{10a}$$

$$b_2=\oint \left[\rho y^2 h+\rho\frac{h^3}{12}\left(\frac{dx}{ds}\right)^2\right]ds, \tag{10b}$$

where h denotes the wall thickness of the beam. The governing system of Eqs. (5) of fourth order requires prescription of two boundary conditions at each edge. For cantilevered beams, the boundary conditions (BCs) are, at the beam root ($z=0$),

$$v_0=\theta_x=0, \tag{11}$$

and at the beam tip ($z=L$),

$$v_0'+\theta_x=0, \tag{12a}$$

$$\theta_x'=0. \tag{12b}$$

III. ALTERNATIVE FORM OF GOVERNING EQUATIONS

Equations (5) and the associated boundary conditions [Eqs. (11) and (12)] can be expressed in terms of $v_0(z,t)$ alone. Having in view the potential usefulness of such a representation, it will be recorded here. Obtainable through the elimination of θ_x in the original governing equations, this new form is given by

$$a_{33}v_0'''-\frac{b_1}{a_{55}}(a_{33}\ddot{v}_0''-b_2\ddot{\ddot{v}}_0)+\frac{1}{a_{55}}(a_{33}p_y''-b_2\ddot{p}_y)+b_1\ddot{v}_0-b_2\ddot{v}_0''-p_y=0, \tag{13}$$

whereas the boundary conditions are

$$v_0=0, \tag{14a}$$

$$v_0'+\frac{1}{a_{55}}\left(v_0'''-\frac{b_1a_{33}}{a_{55}}\ddot{v}_0'+\frac{a_{33}}{a_{55}}p_y'\right)=0 \quad \text{at } z=0 \tag{14b}$$

and

$$v_0''-\frac{b_1}{a_{55}}\ddot{v}_0+\frac{p_y}{a_{55}}=0, \tag{15a}$$

$$a_{33}v_0'''-b_2\ddot{v}_0'-\frac{b_1a_{33}}{a_{55}}\ddot{v}_0'+\frac{a_{33}}{a_{55}}p_y'=0 \quad \text{at } z=L. \tag{15b}$$

Having in view that a_{55} defines the transverse stiffness, consideration in Eqs. (13)–(15) of $a_{55}\to\infty$ yields the Euler Bernoulli counterpart of the bending equations.

It should be remarked that in both formulations (i.e., for both shear deformable and classical bending beam models), fourth-order governing equations are obtained. A similar result obtained within the theory of *solid* beams was reported in Ref. 10.

IV. SOLUTION METHODOLOGY

The goal is to exactly determine the bending frequency response characteristics of thin-walled beams excited by a harmonically time-dependent point load

$$p_y=F_0\delta(z-z_0)\exp(i\omega t). \tag{16}$$

In Eq. (16), $\delta(\ )$ denotes the Dirac distribution while F_0 and ω denote the amplitude and the excitation frequency of the concentrated load, respectively. For evident reasons, the governing system of Eqs. (5) and the associated boundary conditions, Eqs. (11) and (12), will be converted first to a nondimensional form. To this end the following dimensionless quantities are defined:

$$\tilde{v}_0\equiv v_0/L,\quad \eta\equiv z/L,\quad \eta_0\equiv z_0/L,\quad \tilde{t}\equiv\omega_0 t,$$
$$\tilde{\omega}\equiv\omega/\omega_0,\quad \tilde{F}_0\equiv F_0/a_{55}, \tag{17}$$

where $\omega_0(\equiv\beta_0^2(a_{33}/b_1L^4)^{1/2}$, $\beta_0=1.8751)$ is a reference frequency. For a harmonic time-dependent input, due to the linear character of governing equations, the response is also harmonic, of the same frequency.

Upon replacing in Eqs. (5) and BCs (11) and (12) $\tilde{v}_0$ and θ_x as given by

$$\begin{Bmatrix}\tilde{v}_0(\eta;\tilde{\omega})\\ \theta_x(\eta;\tilde{\omega})\end{Bmatrix}=\begin{Bmatrix}V(\eta)\\ S(\eta)\end{Bmatrix}\exp(i\tilde{\omega}\tilde{t}), \tag{18}$$

in terms of the dimensionless variables (17), the governing system and the boundary conditions become

(a) the governing system

$$V_{,\eta\eta}+S_{,\eta}+\tilde{F}_0\delta(\eta-\eta_0)+\frac{a_{33}\beta_0^4\tilde{\omega}^2}{a_{55}L^2}V=0, \tag{19a}$$

$$S_{,\eta\eta}-\frac{a_{55}}{a_{33}}L^2(V_{,\eta}+S)+\frac{b_2}{b_1L^2}\beta_0^4\tilde{\omega}^2S=0 \tag{19b}$$

and

(b) the boundary conditions

$$\text{at } \eta=0,\quad V=S=0, \tag{20}$$

$$\text{and at } \eta=1,\quad V_{,\eta}+S=S_{,\eta}=0. \tag{21}$$

In Eqs. (19)–(21) the differentiation with respect to the nondimensional spanwise coordinate is denoted as $(\ )_{,\eta}\equiv d(\ )/d\eta$. An exact solution to the problem can be obtained via the Laplace transform technique used in the space domain.[11]

Upon applying to Eqs. (19) and (20) the Laplace transform, in conjunction with the transformed counterparts of the BCs at $\eta=0$ [Eqs. (20)], a system of algebraic equations expressed in matrix form is obtained:

$$\begin{bmatrix}g_{11} & g_{12}\\ g_{21} & g_{22}\end{bmatrix}\begin{Bmatrix}\bar{V}\\ \bar{S}\end{Bmatrix}=\begin{Bmatrix}\mu_1\\ \mu_2\end{Bmatrix}+\begin{Bmatrix}V_{,\eta}(0)\\ S_{,\eta}(0)\end{Bmatrix}. \tag{22}$$

Here $\bar{V}\{\equiv\bar{V}(s)=\mathscr{L}(V(\eta))\}$, $\bar{S}\{\equiv\bar{S}(s)=\mathscr{L}(S(\eta))\}$, where s denotes the Laplace transform variable, $V_{,\eta}(0)\equiv dV/d\eta|_{\eta=0}$, while the elements g_{ij} and μ_i are given by

$$g_{11}=s^2+\frac{a_{33}\eta_0^4\tilde{\omega}^2}{a_{55}L^2},\quad g_{12}=s,$$

$$g_{21}=\frac{a_{55}L^2}{a_{33}}s,\quad g_{22}=s^2+\frac{b_2\beta_0^4\tilde{\omega}^2}{b_1L^2}-\frac{a_{55}L^2}{a_{33}},\tag{23}$$

$$\mu_1=-\tilde{F}_0e^{-s\eta_0},\quad \mu_2=0.$$

Upon solving Eqs. (22) for $\bar{V}(s)$ and $\bar{S}(s)$ one obtains

$$\begin{Bmatrix}\bar{V}(s)\\ \bar{S}(s)\end{Bmatrix}=\frac{1}{g}\begin{bmatrix}\mathscr{g}_{11} & \mathscr{g}_{12}\\ \mathscr{g}_{21} & \mathscr{g}_{22}\end{bmatrix}\begin{Bmatrix}-\tilde{F}_0e^{-s\eta_0}+V_{,\eta}(0)\\ S_{,\eta}(0)\end{Bmatrix},\tag{24}$$

where

$$g=g_{11}g_{22}-g_{12}g_{21},\quad \mathscr{g}_{11}=g_{22},\quad \mathscr{g}_{12}=-g_{12},$$

$$\mathscr{g}_{21}=-g_{21},\quad \mathscr{g}_{22}=g_{11}.\tag{25}$$

The inverse Laplace transform of Eq. (24) yields

$$\begin{Bmatrix}V(\eta)\\ S(\eta)\end{Bmatrix}=\begin{bmatrix}G_{11} & G_{12}\\ G_{21} & G_{22}\end{bmatrix}\begin{Bmatrix}-\tilde{F}_0Y(\eta-\eta_0)\\ 0\end{Bmatrix}+\begin{bmatrix}F_{11} & F_{12}\\ F_{21} & F_{22}\end{bmatrix}\times\begin{Bmatrix}V_{,\eta}(0)\\ S_{,\eta}(0)\end{Bmatrix},\tag{26}$$

where

$$G_{ij}=\sum_{m=1}^{M}\left.\frac{\mathscr{g}_{ij}(s)}{dg/ds}\right|_{s=s_m}e^{s_m(\eta-\eta_0)},\tag{27a}$$

and

$$F_{ij}=\sum_{m=1}^{M}\left.\frac{\mathscr{g}_{ij}(s)}{dg/ds}\right|_{s=s_m}e^{s_m\eta}.\tag{27b}$$

Here s_m denotes the mth root of the polynomial g, $M(=4)$ denotes the number of roots of g, while $Y(\,)$ denotes Heaviside's distribution.

Enforcement in conjunction with (26) of boundary conditions at $\eta=1$, Eqs. (21), yields a system of equations for $V_{,\eta}(0)$ and $S_{,\eta}(0)$ given by

$$\begin{bmatrix}d_{11} & d_{12}\\ d_{21} & d_{22}\end{bmatrix}\begin{Bmatrix}V_{,\eta}(0)\\ S_{,\eta}(0)\end{Bmatrix}=\begin{Bmatrix}f_1\\ f_2\end{Bmatrix},\tag{28}$$

where the elements d_{ij} and $f_i(i,j=1,2)$ are given by

$$d_{11}=(F_{11,\eta}+F_{21})|_{\eta=1},\quad d_{12}=(F_{12,\eta}+F_{22})|_{\eta=1},$$

$$d_{21}=F_{21,\eta}|_{\eta=1},\quad d_{22}=F_{22,\eta}|_{\eta=1},\tag{29}$$

$$f_i=\tilde{F}_0[G_{i1,\eta}Y(\eta-\eta_0)+G_{i1}\delta(\eta-\eta_0)]_{\eta=1}.$$

The response functions $\tilde{v}_0(\eta;\tilde{\omega})$ and $\theta_x(\eta;\tilde{\omega})$ corresponding to a given excitation frequency (referred to as frequency response functions) are determined by replacing the solution of Eqs. (28) [i.e., $V_{,\eta}(0)$ and $S_{,\eta}(0)$] into Eqs. (26). The natural frequencies of the composite thin-walled beam are obtained as the roots of the determinantal equation $\det(d_{ij})=0$.

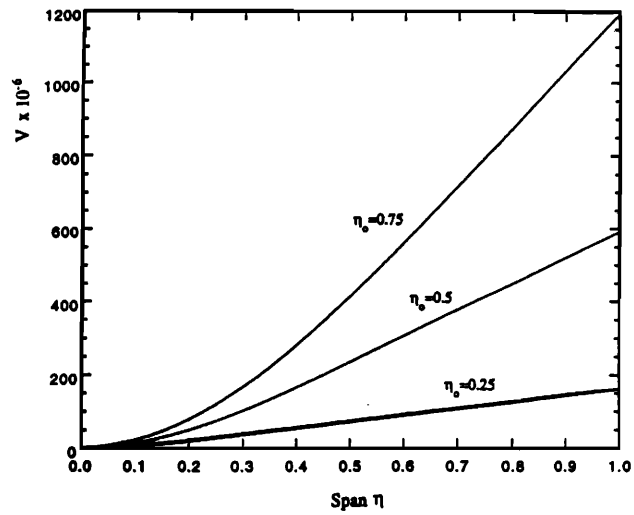

FIG. 2. Distribution along the beam span of $V\times10^{-6}$ for three locations of the loading and for a prescribed $\tilde{\omega}=0.2$.

Knowing the frequency response functions of the system, $\tilde{v}_0(\eta;\tilde{\omega})$ and $\theta_x(\eta;\tilde{\omega})$, the response to any arbitrary time-dependent excitation $F(\eta;\tilde{t})$ can be determined.

In this case, the response quantities $\tilde{v}_0(\eta;\tilde{t})$ and $\theta_x(\eta;\tilde{t})$ can be determined in terms of a convolution integral[12]

$$\begin{Bmatrix}\tilde{v}_0(\eta;t)\\ \theta_x(\eta;t)\end{Bmatrix}=\int_{-\infty}^{+\infty}\begin{Bmatrix}\tilde{v}_0(\eta;\tilde{\tau})\\ \theta_x(\eta;\tilde{\tau})\end{Bmatrix}F(\tilde{\tau}-\tilde{\tau})d\tilde{\tau},\tag{30}$$

where

$$\begin{Bmatrix}\tilde{v}_0(\eta;\tilde{\tau})\\ \theta_x(\eta;\tilde{\tau})\end{Bmatrix}=\mathscr{F}^{-1}\begin{Bmatrix}\tilde{v}_0(\eta;\tilde{\omega})\\ \theta_x(\eta;\tilde{\omega})\end{Bmatrix}=\frac{1}{2\pi}\int_{-\infty}^{+\infty}\begin{Bmatrix}\tilde{v}_0(\eta;\tilde{\omega})\\ \theta_x(\eta;\tilde{\omega})\end{Bmatrix}e^{i\tilde{\omega}\tilde{\tau}}\,d\tilde{\omega},\tag{31}$$

$\mathscr{F}^{-1}$ denoting the inverse Fourier transform operation while $\tilde{\tau}$ denotes a dummy nondimensional time.

Equations (30) and (31) indicate that determination of frequency-response functions constitute a basic step toward determination of the response to arbitrary time-dependent excitations.

V. NUMERICAL ILLUSTRATIONS

The frequency-response characteristics of a single layer cantilevered box-beam constructed of a transversely isotropic material is considered. Its geometrical characteristics are displayed in Fig. 1, whereas the elastic constants of its constituent material are

$$E=206.84\ \text{GPa},\quad E/E'=4,\quad \nu=\nu'=0.25,$$
$$E/G'=5,\quad \rho=7495\ \text{kg/m}^3.\tag{32}$$

Figures 2 and 3 display the distributions of $V(\eta)$ and $S(\eta)$ determined for three locations of $\tilde{F}_0$ along the beam span and for a prescribed $\tilde{\omega}=0.2$.

Figures 4 and 5 depict the distributions of $V(\eta)$ and $S(\eta)$ for three values of the amplitude of the point load $\tilde{F}_0$, located at $\eta_0=0.5$ and for a prescribed $\tilde{\omega}=0.2$.

Figures 6–9 depict the distribution of $V(\eta)$ and of $S(\eta)$

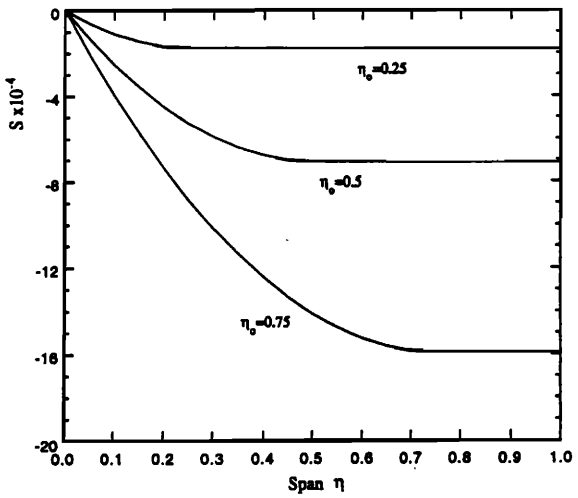

FIG. 3. Distribution along the beam span of $S\times10^{-4}$ for three locations of the loading and for a prescribed $\tilde{\omega}=0.2$.

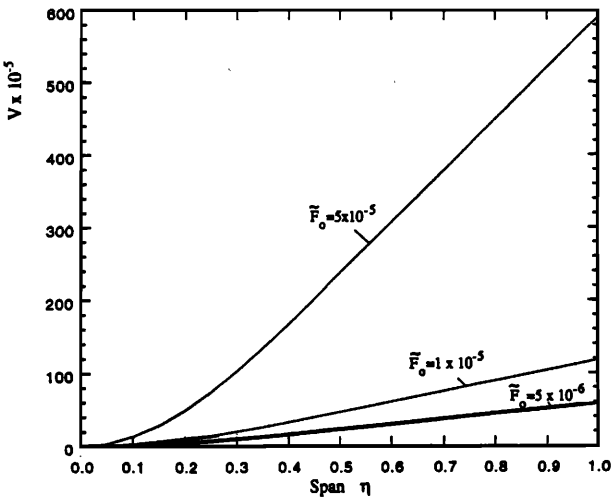

FIG. 4. Distribution along the beam span of $V\times10^{-5}$ for three amplitudes of the loading applied at $\eta_0=0.5$ and for a prescribed $\tilde{\omega}=0.2$.

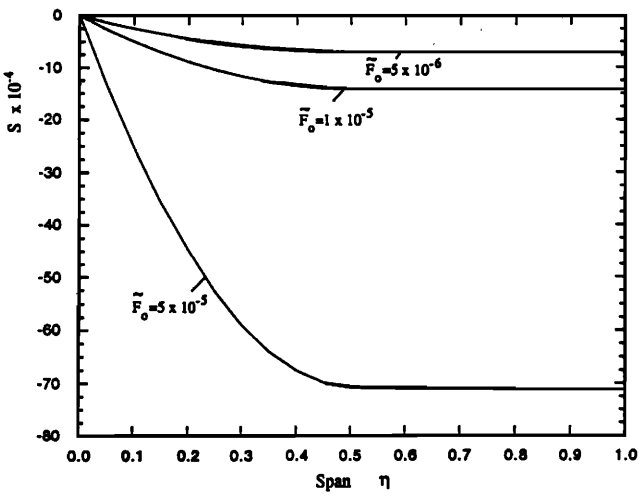

FIG. 5. Distribution along the beam span of $S\times10^{-4}$ for three amplitudes of the loading applied at $\eta_0=0.5$ and for a prescribed $\tilde{\omega}=0.2$.

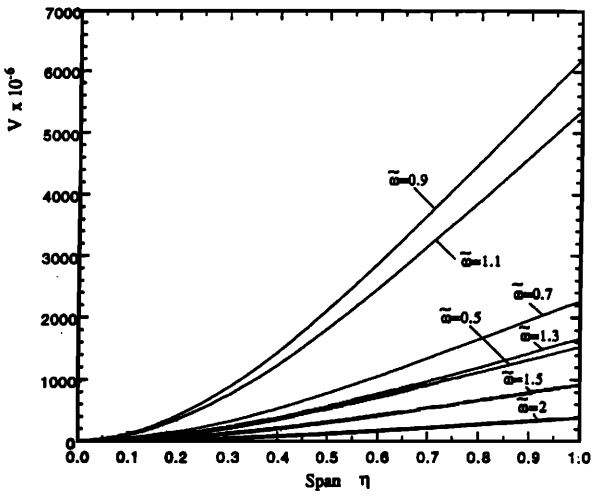

FIG. 6. Distribution along the beam span of $V\times10^{-6}$ for a number of excitation frequencies (of the loading of amplitude $\tilde{F}_0=5\times10^{-6}$ applied at $\eta_0=0.75$).

for a number of external frequency excitations of the concentrated load of amplitude $\tilde{F}_0=5\times10^{-6}$ applied at $\eta_0=0.75$.

Figures 10–12 display the distributions of V at the tip versus excitation frequency ($\tilde{\omega}$) for a loading of amplitude $\tilde{F}_0=5\times10^{-6}$ applied at $\eta_0=0.75$.

The resonance behavior illustrated in Figs. 10–12 can be adaptively controlled as to eliminate its damaging effects. This can be accomplished via a methodology similar to that developed in Ref. 13.

For a full understanding of the trend of variation of $V(\eta)$ and $S(\eta)$ as displayed in Figs. 6–12, it is necessary to point out that the first three eigenfrequencies of the considered structure are

$$\tilde{\Omega}=1,\ 6.16,\ \text{and}\ 16.9.$$

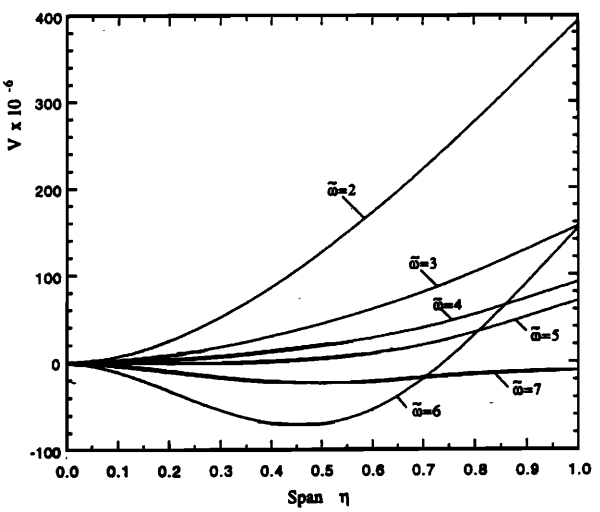

FIG. 7. Distribution along the beam span of $V\times10^{-6}$ for a number of excitation frequencies (of the loading of amplitude $\tilde{F}_0=5\times10^{-6}$ located at $\eta_0=0.75$).

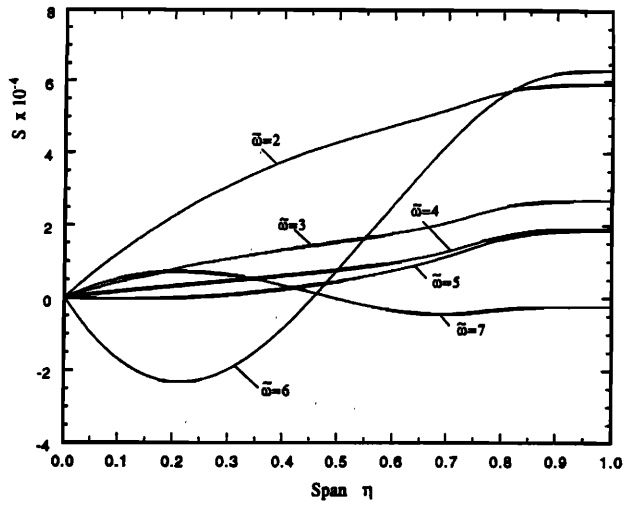

FIG. 8. Distribution along the beam span of $S\times10^{-4}$ for a number of excitation frequencies (of the loading of amplitude $\tilde{F}_0=5\times10^{-6}$ applied at $\eta_0=0.75$).

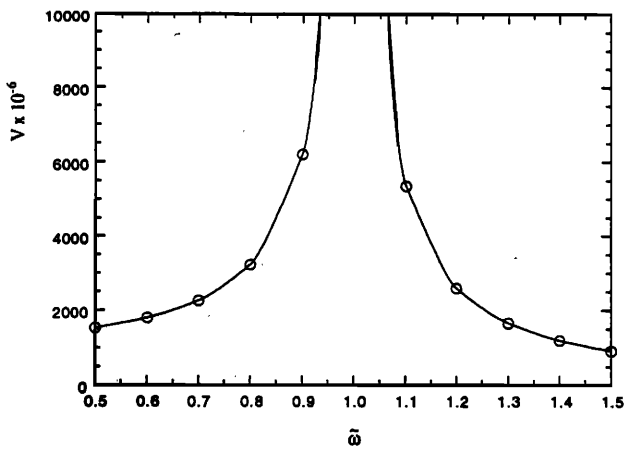

FIG. 10. Distribution of $V\times10^{-6}$ at the tip versus excitation frequency ($0.5\leqslant\tilde{\omega}\leqslant1.5$) for a loading of amplitude $\tilde{F}_0=5\times10^{-6}$ applied at $\eta_0=0.75$.

VI. CONCLUDING REMARKS

A structural model and solution methodology devoted to the study of the bending vibration response of laminated composite cantilevered thin-walled beams of arbitrary closed cross section subjected to a harmonically oscillating concentrated load are presented. The beam model incorporates a number of nonclassical features, such as anisotropy, transverse shear, and secondary warping. The solution methodology which is based upon the Laplace transform technique enables one to determine exactly the frequency-response functions as well as the eigenfrequencies of the system. The numerical illustrations emphasize the role played by the excitation frequency, location along the span, and amplitude of the concentrated load, etc.

The possibility of determining the response in the time domain to an arbitrary time-dependent distributed load was also considered. Finally, it should be pointed out that within a classical beam model (for which an infinite rigidity in

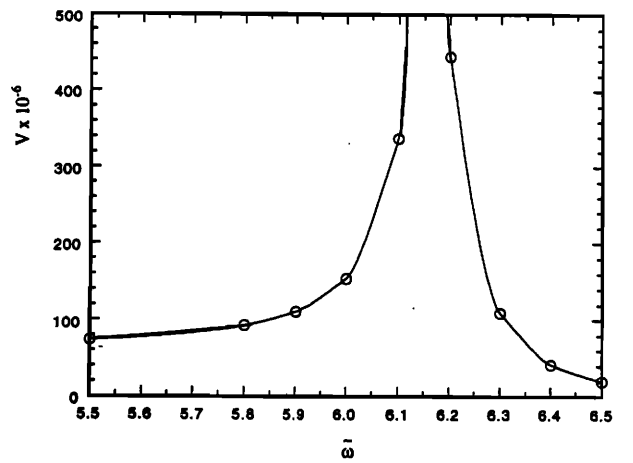

FIG. 11. Distribution of $V\times10^{-6}$ at the tip versus excitation frequency ($5.5\leqslant\tilde{\omega}\leqslant6.5$) for a loading of amplitude $\tilde{F}_0=5\times10^{-6}$ applied at $\eta_0=0.75$.

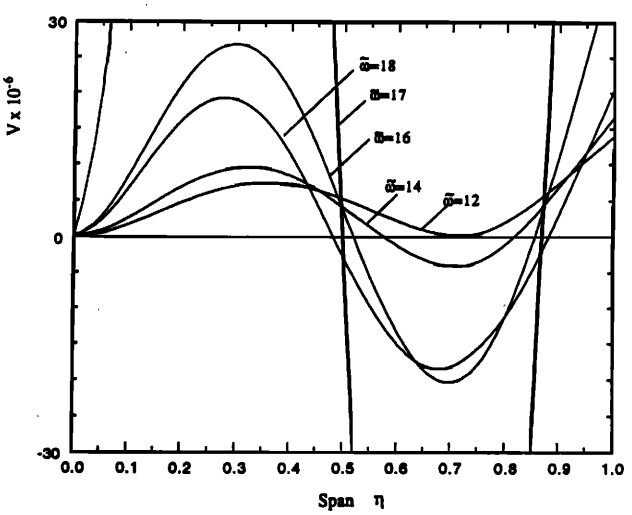

FIG. 9. Distribution along the beam span of $V\times10^{-6}$ for a number of excitation frequencies (of the loading of amplitude $\tilde{F}_0=5\times10^{-6}$ located at $\eta_0=0.75$).

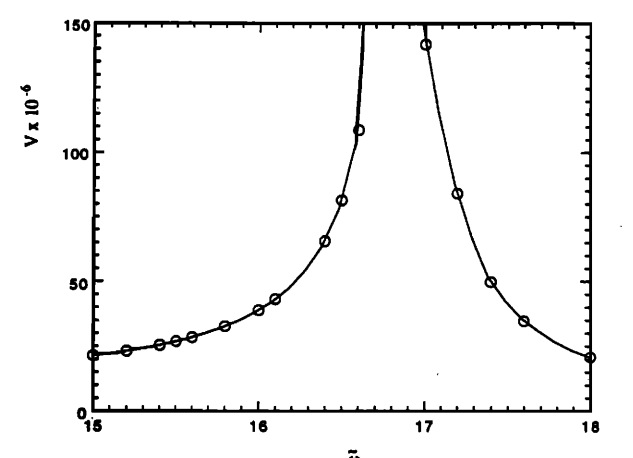

FIG. 12. Distribution of $V\times10^{-6}$ at the tip versus excitation frequency ($15\leqslant\tilde{\omega}\leqslant18$) for a loading of amplitude $\tilde{F}_0=5\times10^{-6}$ applied at $\eta_0=0.75$.

transverse shear is postulated) higher eigenfrequencies would be predicted.[5]

In such a case, the resonance regions corresponding to Figs. 10–12 would be shifted toward higher excitation frequencies. This shows that the inadvertent disregard in the analysis of transverse shear flexibilities featured by the actual beam can result in an overestimation of the resonance frequencies and, consequently, in the underdesign/misuse of such structures exposed to time-dependent excitations.

[1] L. C. Bank and C. H. Kao, "Dynamic response of composite beams," Recent Advances in the Macro- and Micro-Mechanics of Composite Material Structures, AD 13, edited by D. Hui and J. R. Vinson, The Winter Annual Meeting of the 1975 ASME, Chicago, Illinois, Nov.–Dec. 1977.

[2] W. Lee and H. Chao, "Flexural vibration analysis of a loaded double-tapered circular beam with a linearly varying wall thickness," J. Acoust. Soc. Am. **92**, 2260–2263 (1992).

[3] L. Librescu and A. Nosier, "Dynamic response of anisotropic composite panels to time-dependent external excitations," 17th Congress of the International Council of the Aeronautical Sciences, Paper ICAS 90-1.4R, Stockholm, Sweden, 1990, 2134–2144 (1990).

[4] L. W. Rehfield, "Design analysis methodology for composite rotor blades," Proceedings of the Seventh DoD/NASA Conference on Fibrous Composites in Structural Design, AFWAL-TR-85-3094, June, v(a)-1–v(a)-15 (1983).

[5] L. Librescu and O. Song, "Behavior of thin-walled beams made of advanced composite materials and incorporating non-classical effects," Appl. Mech. Rev. **44**, 174–180 (1991).

[6] O. Song and L. Librescu, "Free vibration of anisotropic composite thin-walled beams of closed cross-section contour," J. Sound Vib. **167**, 129–147 (1993).

[7] L. Librescu and O. Song, "On the static aeroelastic tailoring of composite aircraft swept wings modeled as thin-walled beam structures," Compos. Eng. **2**, 497–512 (1992).

[8] A. Gjelsvik, *The Theory of Thin Walled Bars* (Wiley, New York, 1981).

[9] L. Librescu, *Elastostatics and Kinetics of Anisotropic and Heterogeneous Shell-Type Structures* (Noordhoff, The Netherlands, 1975).

[10] G. Karpouzian and L. Librescu, "A comprehensive model for anisotropic composite aircraft wings suitable for aeroelastic analyses," J. Aircraft **31**, 703–712 (1994).

[11] L. Librescu and S. Thangjitham, "Analytical studies on static aeroelastic behavior of forward-swept composite wing structures," J. Aircraft **28**, 151–157 (1990).

[12] A. V. Oppenheim, A. S. Willsky, and I. T. Young, *Signals and Systems* (Prentice-Hall, Englewood Cliffs, NJ, 1983).

[13] O. Song, L. Librescu, and C. A. Rogers, "Application of adaptive technology to static aeroelastic control of wing structures," AIAA J. **30**, 2882–2889 (1992).